The Coupled-Cavity Transmission Maser-Engineering Design

F. E. GOODWIN, MEMBER, IEEE, J. E. KIEFER, MEMBER, IEEE AND G. E. MOSS, MEMBER, IEEE

Summary—The experimental design of an *X*-band microwave maser amplifier which uses a new type of slow-wave circuit is described. A detailed theoretical analysis of the circuit is presented in a companion paper [1]. The slow-wave circuit consists of a cascade of iris-coupled ruby resonators separated by garnet isolators. This unit provides significant reduction in size and weight over previously reported maser slow-wave circuits.

The microwave properties of the solid ruby resonator are treated in detail, and the passive bandwidth of the single transmission cavity and its relation to the iris susceptance are shown. Experimental techniques involved in obtaining and measuring precise iris susceptance are presented. A step-by-step procedure for designing an amplifier having a given gain and tuning range is also presented.

Typical performance characteristics include a gain of 30 db, instantaneous bandwidth of 25 Mc, and a noise temperature of 15°K. An electronic tuning range of 200 Mc has been achieved in one configuration with a 20 db gain and a 25-Mc bandwidth. The weight of the maser-dewar unit, filled with 6 liters of helium for 24 hours of operation is less than 40 pounds. The design of the dewar enables the cryogenic system to work over a wide range of vertical angles, thus facilitating the use of the maser at the feed of a large steerable antenna.

I. Introduction

SOON after the first generation of solid-state maser amplifiers were developed, it became apparent that the instability associated with these reflection-type cavity devices would prevent their use for many applications. The benefits derived from the very low noise were reduced by the instability and complexity of the maser and the associated cryogenics. With the development of the traveling-wave maser, greater stability was achieved, and, in addition, great improvements in gain-bandwidth product were obtained. To date, operating traveling-wave masers which utilize slow-wave structures are of four types: the comb structure [2], the meander line [3], the Karp structure [4], and the coupled resonant cavity structure. One of these, the comb-structure maser amplifier, has been developed by several laboratories.

This paper reports on the coupled resonant cavity type maser developed at this laboratory. The primary advantage of this type of structure over the others is its inherent smaller size while it still yields comparable or improved performance characteristics. This reduction in size may be seen to be possible by considering the four basic structures shown in Fig. 1. Each of these structures must be oriented with the static magnetic field in a particular way. To permit unilateral absorption or isolation, the ferromagnetic element is placed in the region of a circularly polarized RF magnetic field, where the static magnetic field must then be perpendicular to the RF field. This requirement follows directly from [5], [6]

$$\frac{d\overline{M}}{dt} = \gamma(\overline{M} \times \overline{H})$$

where $\overline{M}$ is the magnetization, $\overline{H}$ is the magnetic field and γ is the gyromagnetic ratio. The comb structure, meander line and Karp structure are similar in that the plane of RF circular polarization is perpendicular to the plane of the structure. It is thus necessary to orient the static magnetic field parallel to the plane of these structures. However, the waveguide filter structure has the circular RF polarization in the plane of the waveguide and thereby permits the static magnetic field to be directed perpendicular to the plane of the structure. This is a very real advantage over the other types of structures in that the magnet gap length may be considerably reduced thus permitting a much smaller magnet to be used to furnish the necessary field. The static field for an *X*-band coupled-cavity type maser is provided by a small permanent magnet weighing 10 to

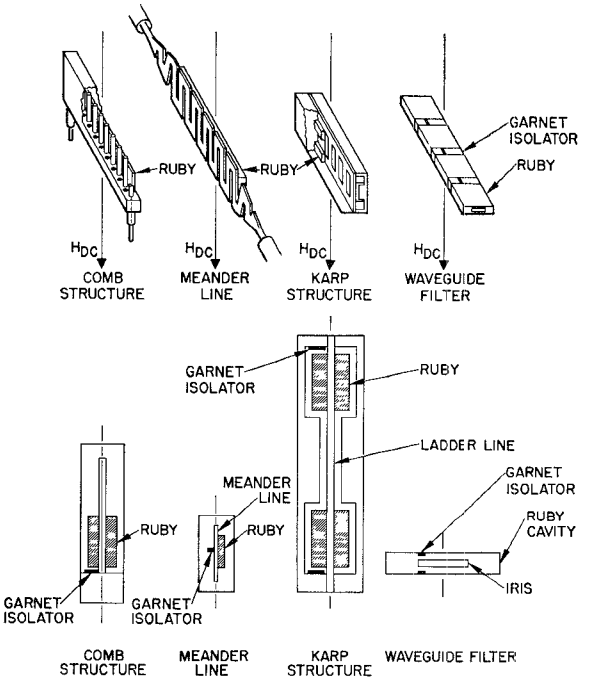

Fig. 1—Four basic traveling-wave maser structures.

Manuscript received October 15, 1963; revised received February 24, 1964.

The authors are with Hughes Research Laboratories, Malibu, Calif.

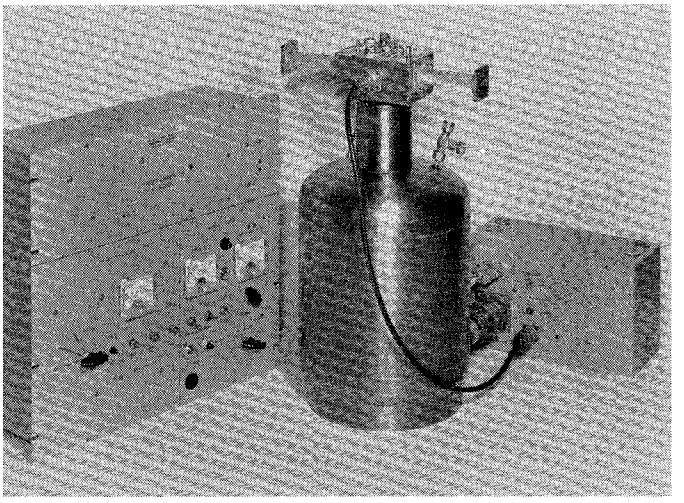

Fig. 2—Complete maser amplifier.

20 ounces which is fixed directly to the maser structure. The relative smallness of the magnet permits it to be cooled along with the maser without excessive expenditure of liquid helium. This type of structure can be readily adapted to use a superconducting magnet, but it has been found that the fields required for operation at *X*-band frequencies may be more easily provided by a permanent magnet.

The elimination of the large magnet facilitates the design of the maser-dewar unit to fulfill practical operating requirements for size, weight and variable angular orientation. In many systems these requirements are imposed by the necessity for locating the maser very close to the feed of a large steerable antenna. Design features of the liquid helium dewar allow operation at all elevation angles encountered while fixed to a steerable antenna. Fig. 2 illustrates the complete maser along with its associated control unit. The dewar, as shown in Fig. 2 (and in Fig. 15), is capable of maintaining the maser at the operating temperature of 4.2°K for over 24 hours with a 6-liter charge of liquid helium.

Closed cycle refrigerators capable of liquid helium temperatures are becoming less expensive and more reliable. These are finding ready application to maser systems where liquid helium availability and storage is a problem. The coupled-cavity maser discussed in this paper has been designed to be readily adaptable to a liquid helium refrigerator.

II. Maser RF Assembly

The maser RF assembly (illustrated in Fig. 3) includes an input-output and pump waveguide flange block, Fiberglas heat exchanger tube and maser unit. The configuration of the heat exchanger tube is such that the escaping helium vapor is forced to flow in contact with the neck tube of the dewar. The space between the waveguides and inside the Fiberglas tube is filled with foamed epoxy to prevent undesirable circulation of gas. The signal input and output waveguides are made of either stainless steel or metallized Fiberglas. At the bottom of the neck, where the waveguide joins the maser, the waveguide is transformed into a solid, alumina-filled waveguide by means of a matching transition. The design of the matching device is considered in Section IV and illustrated in Fig. 9. The dielectric-filled waveguide serves the following three purposes: 1) to keep liquid helium and frozen gases out of the waveguide in the bath, thereby preventing mismatches and instability, 2) to reduce the line impedance to that of the active coupled-cavity filter (the maser amplifying structure) and 3) to reduce the physical size.

The coupled-cavity structure consists of a number of transmission-type cavities which are in cascade and separated from each other by interstage garnet isolators. Pump power is brought into the cavities through a pump distribution waveguide circuit which lies adjacent to the coupled cavities. Each cavity has a pump slot in its side, and the cavities form a slot array for the pump power. Both resonant and nonresonant pump arrays have been used successfully. The arrangement of the structure is shown in disassembled form in Fig. 4.

The magnetic field for the maser is provided by a small Alnico V permanent magnet located within the dewar. Carefully shaped [7] Armco pole pieces assure the required high degree of homogeneity of field (see Fig. 5). A trimming coil mounted on the magnet allows small variations of the field magnitude necessary for initial adjustment and for fine frequency tuning of the maser. Two modes of control of the magnitude of the field are possible. By applying regulated direct current to the trimming coil, the field magnitude may be continuously varied. If long time operation at a given field is required, the field magnitude may be fixed by discharging a charged capacitor through the trimming coil. Varying the charging voltage varies the final field to which the magnet is charged, and when the desired field is established, the magnet control may be turned off. (This feature is desirable because it removes the dependence of the magnetic field stability, and thus the gain stability of the maser from the direct current supply.) Also, by eliminating the continuous current through the trimming coil, a significant heat load to the liquid helium bath is removed.

A superconducting lead shell surrounding the maser assembly provides the magnetic shielding found necessary to eliminate the gain fluctuations of the maser due to variations in external magnetic fields.

One electrical advantage of the waveguide filter, or coupled-cavity maser, is that the structure pass band may be reduced arbitrarily without changing the front-to-back ratio of the isolators. Since the isolators are not in a region of high RF field, the net forward loss remains small even when structure pass bands are reduced to 0.2 percent. The reduced pass band, however, increases

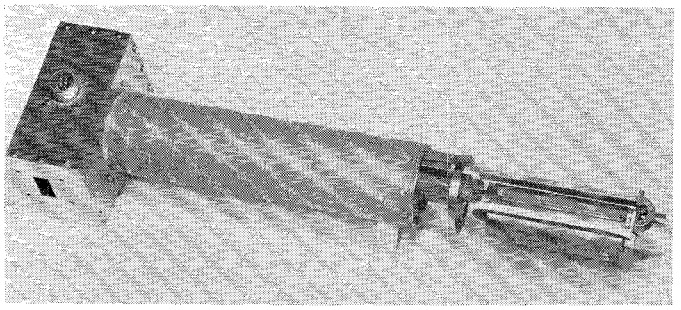

Fig. 3—Maser RF assembly.

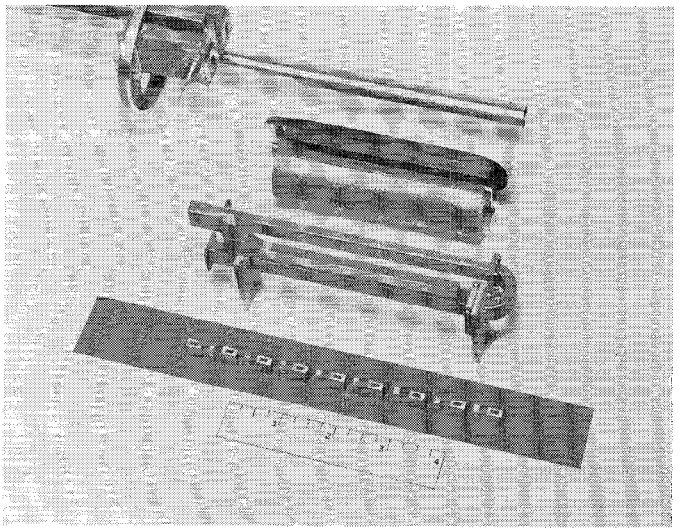

Fig. 4—Disassembled RF structure.

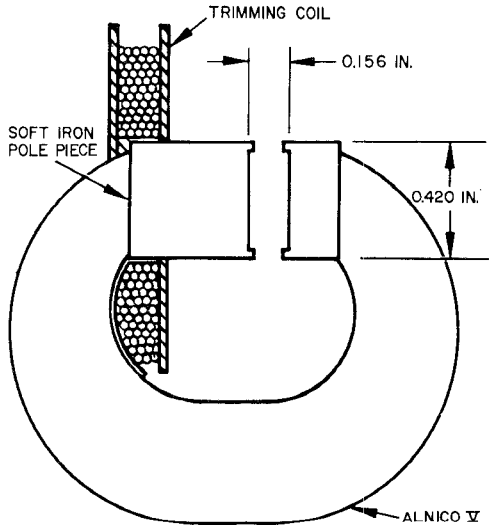

Fig. 5—Cross section of maser magnet.

the gain as shown by the approximate relationship [8]

$$G(dB) \simeq \frac{8.6M}{Q_m \overline{BW}},$$

where

$M \equiv$ number of resonators
$Q_m \equiv$ magnetic Q of material
$\overline{BW} \equiv$ structure pass band (fractional).

With an arbitrarily narrow pass band, high net gain may be achieved by using maser materials of relatively high magnetic Q, such as would be the case when operating a ruby maser at temperatures higher than that of liquid helium. It has been shown [9] that amplification can be achieved in a ruby reflection-type-cavity maser at temperatures as high as 77°K. Thus, it would be possible to extend the operation of the multiple-resonator transmission device to higher temperatures, although the required pump power may set the upper limit to practical operating temperature. For the purposes of this paper, however, we consider only operation at 4.2°K, the temperature of liquid helium at 1 atmosphere of pressure, where the over-all performance capabilities of the coupled-cavity transmission maser are the most practical.

III. Microwave Properties of the Solid Ruby Resonator

Resonator Frequency

The resonant cavities which form the slow-wave structure consist of rectangular papallelepipeds of ruby constructed to be resonant in the TE_{011} mode. Silver plating is used to form the conductive wall of the cavity. To form the coupling irises of the resonator this plating is removed from precisely determined areas. A filling factor of unity is assured with this type of construction as well as high stability of the cavity resonant frequency. Two dimensions of the resonator are fixed by the structure cross section, while the third (the dimension parallel to the direction of propagation through the structure) is used to fix the resonant frequency.

To determine the resonant frequency of the cavity, the effective dielectric permittivity of ruby for this configuration must be known. Ruby is an electrically anisotropic crystal and as such has a tensor dielectric permittivity. In addition, ruby is uniaxial, which means that the dielectric permittivities are such that $\epsilon_x = \epsilon_y \neq \epsilon_z$ where the z direction is parallel to the optical axis. ϵ_x, ϵ_y and ϵ_z are called the principal dielectric permittivities of the crystal. For clarity, let $\epsilon_z = \epsilon_\parallel$ and $\epsilon_x = \epsilon_y = \epsilon_\perp$. The principal dielectric permittivities for ruby have been measured at 9 kMc and are shown as a function of temperature in Fig. 6. The effective refractive index n of ruby may be determined by the ellipsoid of revolu-

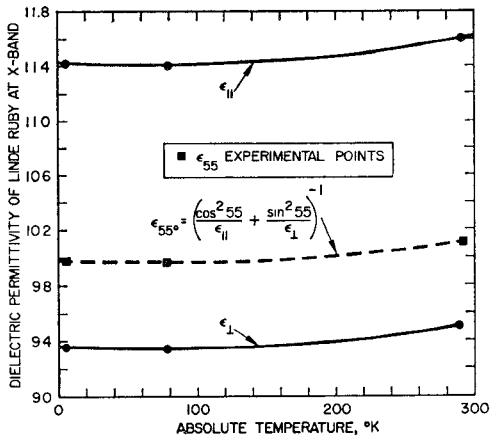

Fig. 6—Relative dielectric permittivity of Linde ruby as a function of temperature.

tion about the optical axis

$$\frac{1}{n^2} = \frac{\cos^2\theta}{n_\parallel^2} + \frac{\sin^2\theta}{n_\perp^2}$$

where θ is the angle between the electric vector and the optical axis. Therefore, the effective dielectric permittivity ϵ for ruby is given by

$$\frac{1}{\epsilon} = \frac{\cos^2\theta}{\epsilon_\parallel} + \frac{\sin^2\theta}{\epsilon_\perp}.$$

The resonators are normally constructed such that $\theta = 55°$; the effective dielectric permittivity for this configuration is also given by Fig. 6. The length of the ruby resonator can thus be found for a predetermined unloaded resonant frequency f_u and width a from the relation

$$\text{ruby length} = \frac{c/2f_u}{\sqrt{\epsilon - \left(\frac{c}{2f_u a}\right)^2}} \text{ cm} \qquad (1)$$

where $c = 3 \times 10^{10}$ cm/sec.

The relative impedance of the coupling irises pulls the resonant frequency of the cavity to some loaded frequency f_0. The fractional deviation δ_f is given by [10]

$$\delta_f = \frac{f_0 - f_u}{f_u} \cong \left(\frac{b}{2Q_L}\right) \qquad (2)$$

where Q_L is the loaded Q of the cavity and $b = B/Y_0$, the normalized susceptance of the coupling irises which are assumed to be identical.

B. Loaded Q

The loaded Q of the cavity has special significance since the power gain G of the maser depends upon the ratio of this quantity to the magnetic quality factor of the maser material Q_m [11]. For any given set of operating conditions, the magnetic Q is optimized and remains fixed. Thus the gain depends on the loaded Q, and therefore on iris susceptance. The conventional expression for the loaded Q of a waveguide resonator is given by [12]

$$\overline{(BW)}^{-1} = Q_L = \frac{b^2 + 1}{4\left[1 - \left(\frac{f_c^2}{f_0}\right)\right]} \tan^{-1}\left(\frac{2b}{b^2 - 1}\right) \qquad (3)$$

where f_0 is the cavity resonant frequency and f_c is the waveguide cut-off frequency.

Another expression for loaded Q, which is obtained from transmission line theory is

$$\overline{(BW)}^{-1} = Q_L = \frac{\pi - 2\tan^{-1}\left(\frac{1}{b}\right)}{\left[1 - \left(\frac{f_c}{f_0}\right)^2\right] \ln\left[\left(\frac{2}{b}\right)^2 + 1\right]} \qquad (4)$$

for $b > 2$.

For the middle of the waveguide band and large b, (3) and (4) reduce to $\pi b^2/2$. Eq. (4) and its reciprocal, fractional bandwidth $\overline{BW}$, are plotted in Fig. 7 for several values of (f_c/f_0). It can be seen that there is excellent correlation with experimental $\overline{BW}$ points.

C. Magnetic Q

The magnetic Q is defined as the reciprocal of the imaginary part of the paramagnetic susceptibility χ'' and is given by [9]

$$Q_m = \frac{1}{\chi''} = \frac{h\nu_s}{8\pi(n_2 - n_1)\langle\mu^2\rangle F}$$

where h is Planck's constant, ν_s is the signal frequency' n_1 and n_2 are the number of ions in spin states 1 and 2' $\langle\mu^2\rangle$ is the average squared dipole moment of the maser transition and F is the cavity filling factor. For the particular case of the symmetric or four-level "push-pull" mode, Q_m reduces to

$$Q_m = \frac{kT\Delta\nu_m}{2\pi N_0\langle\mu^2\rangle(\nu_p - \nu_s)}, \qquad (5)$$

where k is Boltzmann's constant, T is the absolute temperature, $\Delta\nu_m$ is the line width of the transition, N_0 is the number of maser ions per cm^3 and ν_p is the pump frequency which is fixed by ν_s.

Eq. (5) which is plotted in Fig. 8 represents the minimum or best possible value of Q_m. In practice, this value is never realized because it is degraded by several factors, such as broadening of the paramagnetic line width by inhomogeneous magnetic field or by crystal imperfections, incomplete saturation of pump transition (incomplete inversion), lower than unity filling factor, or local heating of the ruby by high pump power.

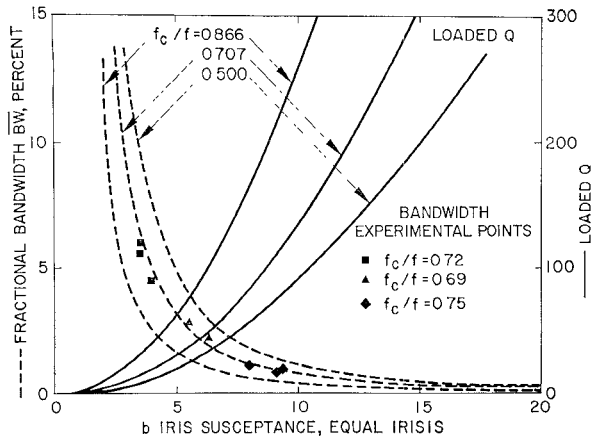

Fig. 7—Passive bandwidth of transmission cavity as a function of iris susceptance (equal irises).

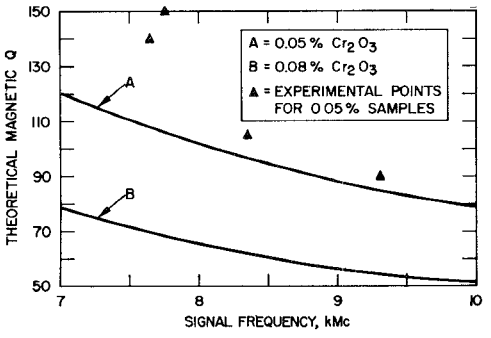

Fig. 8.—Magnetic Q as a function of frequency for ruby at $\theta = 54.7°$.

D. Iris Susceptance Measurements

We have seen that the gain of the maser and relative bandwidth of the ruby filter structure depend upon the iris susceptance. The key to this maser design, therefore, is the achievement of precise iris susceptances. A simple and accurate method for attaining precision irises is to remove the silver plating from the area of the coupling iris by fine sandblasting through a thin metal template of a predetermined size.

The shape of the iris is a critical factor in coupling between the rubies because a favorable field distribution in the isolator must be maintained. The optimum shape of the iris is rectangular with the E dimension (height of the iris) about half that of the ruby. The width of the iris then determines its susceptance. Two methods used for measuring the iris susceptance are the following:

1) *The Reflection Coefficient Method*—The standard method of measuring a susceptance is by measuring the reflected power from an iris. In this case, since dielectric filled waveguide is used, great care must be taken that the iris is backed up by a matched termination. The reflection coefficient ρ is related to the iris susceptance by

$$\rho = \left[\left(\frac{2}{b}\right)^2 + 1\right]^{-1/2} = \left(\frac{P_{\text{reflected}}}{P_{\text{incident}}}\right)^{1/2}.$$

This method is satisfactory for determining the susceptance of an iris on the thin metal template used as a pattern for cutting irises on the rubies.

2) *The Del Method*—After the iris has been cut on a ruby, it is possible to determine its susceptance by measuring the detuning or frequency pulling introduced by the reactive nature of the iris. The resonant frequency of the cavity with the iris shorted is compared with the resonant frequency with the iris open circuited. A quarter wavelength ruby shorted at the iris end provides the open circuit. The relation of the amount of frequency detuning δ_f to the iris susceptance of a conventional half-wave transmission line is given by

$$\delta_f = \frac{f_0 - f_u}{f_u} = \frac{1}{\pi}\tan^{-1}\left(\frac{1}{b}\right),$$

which for the case of waveguides becomes

$$\delta_f = \frac{f_0 - f_u}{f_u} = \frac{1}{\pi}\left[1 - \left(\frac{f_c}{f_0}\right)^2\right]\tan^{-1}\left(\frac{1}{b}\right).$$

IV. Broad-Band Impedance Match into a Dielectric Filled Waveguide

Relatively good broad band RF matches from a standard waveguide into a dielectric-filled waveguide can be obtained with the transition shown in Fig. 9 [13] on the next page. For frequency independent impedance match, the height of the two waveguides must be equal at the junction and their widths must be related by

$$\frac{a_1}{a_2} = \sqrt{\frac{\epsilon_2}{\epsilon_0}}$$

where $\epsilon_2/\epsilon_0 = 9.4$ for alumina. The optimum stub diameter is 0.8 a_2, and its optimum position is $a_2/2$ from the junction. The depth of the stub is adjusted for best match. A typical VSWR of 1.16 or less can be obtained over a 25 per cent band with the X-band device.

V. The Coupled-Cavity Filter Structure

O'Meara [1] has described the equivalent network of the ruby cavity and has analyzed the combined M-cavity amplifier network. His analysis yielded essential design relations and optimum values of parameters. In this and the sections that follow, repeated reference is made to his analysis of the isolator-iris effective line length, the optimum isolation for general M-cavity system and the gain-frequency functions. Computed data from this analysis of a 15-cavity maser amplifier are compared with experimental results.

A. Passive, Nonisolated Structure

The bandwidth $\overline{BW}$ of a single passive-transmission ruby cavity has been given as a function of iris susceptance [(4)] and plotted in Fig. 7. When the number of cavities M of the system is increased from 1, it can be shown that the structure bandwidth decreases to a minimum for $M = 2$, increases for $M > 2$, and approaches that of a single cavity again for larger M. Therefore,

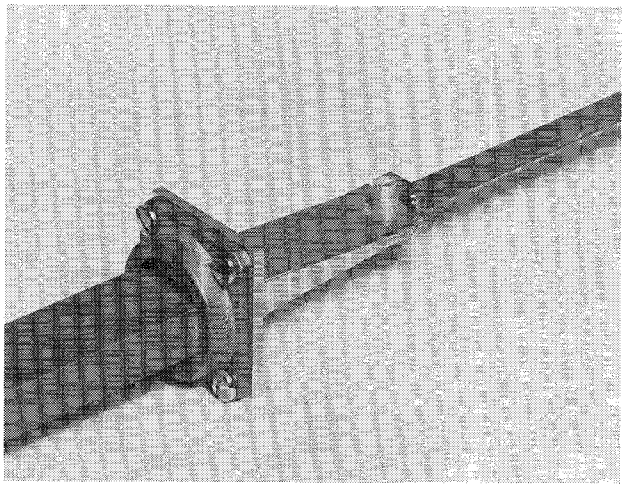

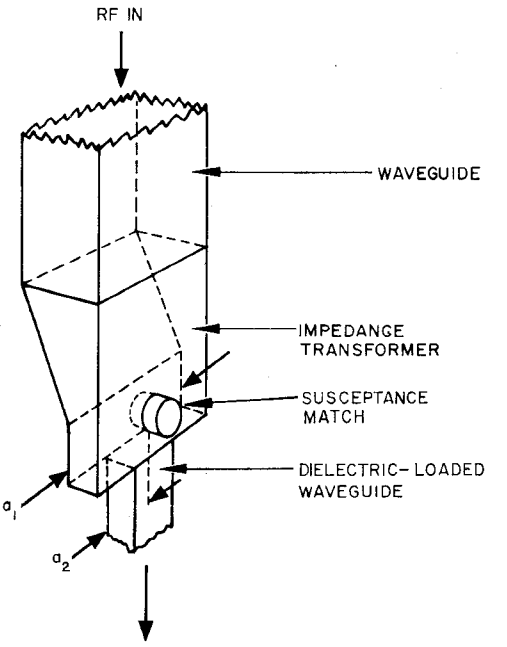

(a) (b)

Fig. 9—Broad-band impedance transition from standard to dielectric-filled waveguide.

(4) holds for large M and is nearly correct for $M=4$. Experimental results agree with this prediction to a high degree of accuracy for $M>4$.

The measured phase-frequency diagram for a passive 15-resonator structure is given in Fig. 10 (opposite) where $\beta l/\pi$ is the normalized phase shift per cavity. Fig. 10 also illustrates the calculated single cavity bandwidth $\overline{BW}$ compared with both the measured reflected and the transmitted power over the region of the pass band. It can be seen that the bandwidth of the 15-resonator filter is 425 Mc, or slightly less than the calculated $\overline{BW}=440$ Mc. A good passive filter characteristic is necessary for a good active maser amplifier. This of course requires precise control of the iris susceptance and ruby resonator center frequencies.

B. The Isolator

Three important functions of the isolators are directly related to their physical length. First, the isolator must be long enough to provide sufficient separation between cavities so that the mutual coupling between irises is small. For this case, the net susceptance of the coupling element is twice the susceptance of a single iris. This gives the desired filter characteristic for the maser structure.

The second function of the isolator length is related to the symmetry of the structure pass band. It can be shown [1] that a symmetric pass band may be obtained if quarter-wave coupling between elements is provided. The electrical length of each isolator βl must then satisfy the requirement

$$\beta l + 2 \tan^{-1} b = \pm \frac{\pi}{2}$$

where b is the iris susceptance.

The third function of the isolator electrical length is to provide isolation to the active maser amplifier. The optimum isolation, discussed below, is determined by the gain of the individual cavities, and since the isolation is nearly a linear function of length, the optimum length is established.

C. Active Isolated Structure

When the structure is cooled to liquid helium temperatures and pump power is provided to the rubies, the filter becomes active. In order for the filter to provide stable gain, isolation is required. The minimum interstage isolation necessary to prevent oscillation, which was determined by the partially invariant method [1], is approximately twice the single cavity gain. Because large ripple in the gain-frequency response is undesirable, an isolation of twice the single cavity gain is regarded as a lower bound. A maximally flat gain-frequency response is obtained with an interstage isolation of approximately three times the gain per stage. In practice, a value of two and one-half is adequate to produce smooth gain characteristics. The optimum value is not a linear function of the gain per stage, so the curves should be consulted for exact values (O'Meara [1], Fig. 6).

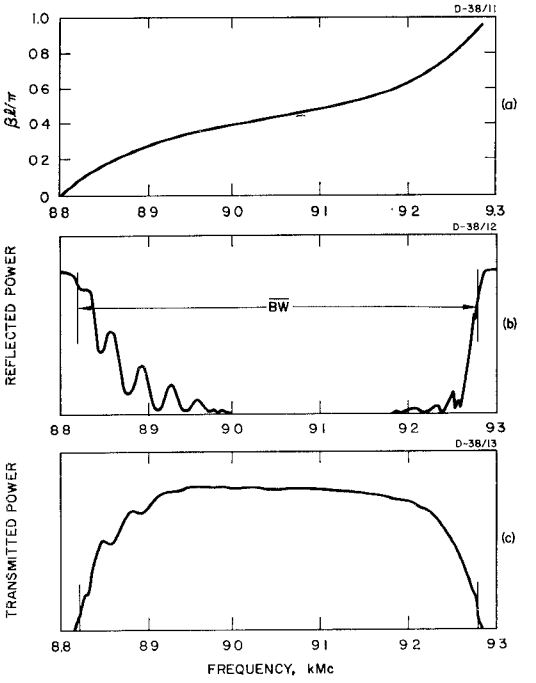

Fig. 10—Passive transmission and reflection characteristics of the 15-cavity maser.

D. Tunability and Gain Characteristic

The fractional active (tunable) bandwidth of an M-resonator maser amplifier is given to a good approximation by the relation [1]

$$B_r \doteq \frac{1}{Q_m}\left(\frac{g_{os}}{g_{oe}}\right)\frac{(1+H)^{(1-M)/M}}{(g_{os}-1)} \tag{6}$$

where g_{oe} is the effective single cavity voltage gain, g_{os} is the isolated single cavity voltage gain, and H is the round trip attenuation per isolator as a voltage ratio. The isolator attenuation is assumed to be that which yields a maximally flat structure response. The product B_rQ_m computed as a function of M for several values of total amplifier gain is given in Fig. 11. The passive structure bandwidth $\overline{BW}$ for large M may be determined from the single cavity gain by using the relationship [11].

$$g_{os} = \frac{\overline{BW}Q_m}{\overline{BW}Q_m - 1}. \tag{7}$$

In practice the gain per cavity is reduced by feedback through the noninfinite isolator. The theoretical gain loss per stage as a function of the isolated single cavity gain with the interstage isolation as the parameter is shown by the curves of Fig. 12. The effect of interstage isolation on the active bandwidth of the maser is illustrated by the curves of Fig. 13 which show the gain-frequency characteristics of a 15-resonator maser for a series of isolator attenuation values. It has also been found experimentally that the minimum isolation required for stable maser gain results in an active bandwidth which is reduced nearly 50 per cent from that of the passive structure.

The signal frequency of the maser amplifier, which is determined by the 2→3 transition of the ruby spin system, is a function of the magnetic field. It is plotted in Fig. 14 for the frequency interval from 7 to 10 Gc. The amplification band may be tuned either up or down in frequency by increasing or decreasing the magnetic field strength. The exact eigenvalues for either the signal or pump frequency can be obtained from the spin-Hamiltonian or from published tables [14].

E. Amplifier Bandwidth

The instantaneous amplifier (3 db) bandwidth is determined by the shape of the ruby line and is given by the expression for a conventional traveling-wave maser

$$\text{Amplifier bandwidth} \equiv \Delta\nu_m\sqrt{\frac{3}{G_{dB}-3}}.$$

F. Isolator Alignment and Tracking

The ferromagnetic resonant frequency of a ferrite depends upon the magnitude of the applied static magnetic field, the magnetic properties of the material and the size and shape of the specimen being considered. Kittel has shown [5] that the resonant frequency ω of a ferrite sample in the form of an ellipsoid with principal axes parallel to the x, y, z coordinate axes is given by

$$\omega = \gamma\{[H_z + (N_y - N_z)M_z][H_z + (N_x - N_z)M_z]\}^{1/2}$$

where N_x, N_y and N_z are the demagnetizing factors which are functions of this size and shape of the sample, M_z is the saturation magnetization of the material and

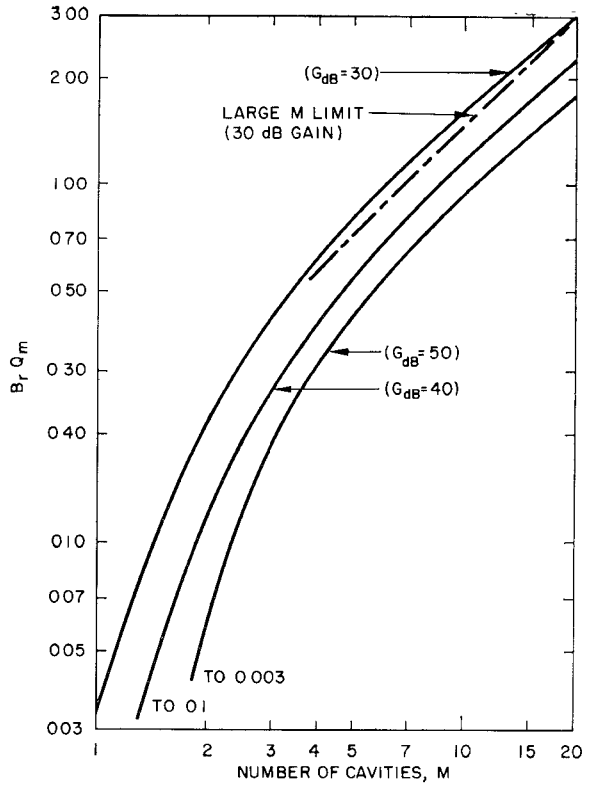

Fig. 11—Some approximations to tunable percentage bandwidth as a function of a number of cavities with over-all gain as the parameter.

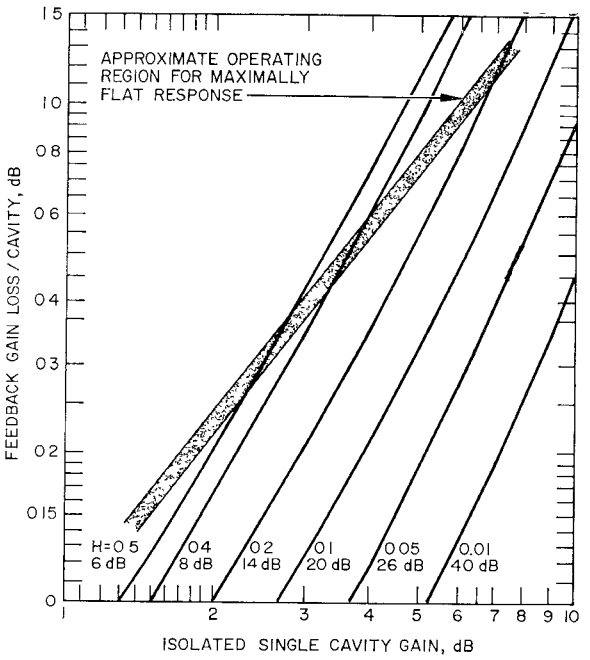

Fig. 12—Inverse feedback gain loss as a function of single cavity gain with M as a parameter.

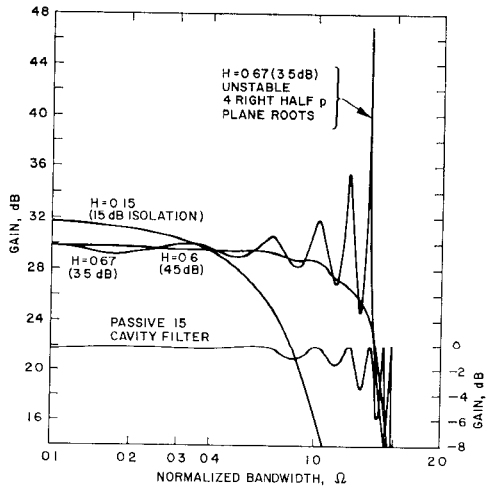

Fig. 13—Theoretical frequency response for a 15-cavity maser, $g_{os}=1.288$.

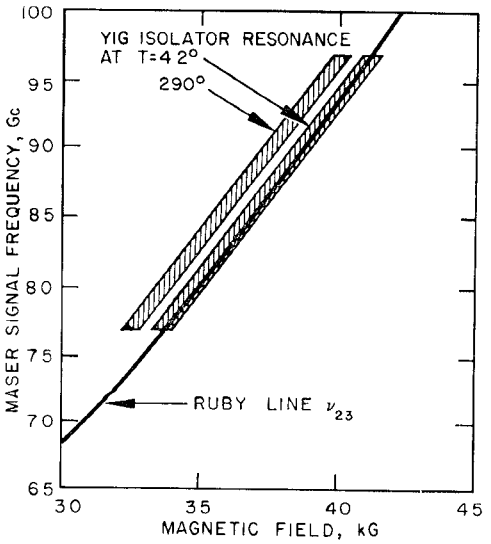

Fig. 14—Ruby γ_{23} signal transition and isolator tracking as a function of magnetic field ($\theta=54.7°$).

H_z is the static magnetic field. γ is the magneto-mechanical ratio which for electron spin is numerically 2.8 Mc/G.

The ferrite best suited for use as the maser isolator material was found to be polycrystalline yttrium-iron-garnet (YIG) which has a saturation magnetization of about 2200 G at 4.2°K. The ferrite is in the form of a rectangular parallelepiped and is located in the plane of circularly polarized RF magnetic field of the TE_{01} propagating mode of the solid alumina waveguide.

In designing the isolators, it was necessary to adjust the demagnetizing factors of the ferrite to the values which allow the ferromagnetic resonance to coincide with the paramagnetic resonance of the ruby as a function of the applied static magnetic field. For a narrow frequency of operation, this is a relatively simple matter. Since the paramagnetic resonance of ruby nearly follows the Larmour condition $\omega=\gamma H$, it can be seen from the Kittel equation that the isolator absorption frequency can be made to follow the ruby line over a wide frequency range only if $N_x=N_y$ or if N_x and N_y are very small relative to N_z.

Fig. 14 shows the absorption line (cross-hatched area) of a typical wide band isolator at both room temperature and at 4.2°K.

VI. Traveling-Wave Maser Design Procedure

The performance specifications of the maser amplifier determine its configuration. Specifications which are particularly relevant are listed in Table I, along with the parameters to be determined. The design data for a tunable X-band maser which is now operational is given in Table II.

TABLE I

Performance Specifications and Essential Parameters of Maser Amplifier

Amplifier Specifications	Parameters to Be Determined
Net gain	Electronic gain G_{db}
Center frequency	Magnetic Q
Tunable bandwidth B_r	Number of cavities M
	Passive bandwidth $\overline{BW}$
	Iris susceptance b
	Interstage isolation H
	Isolator length θ_{is}
	Magnetic field
	Pump frequency

TABLE II

Design Data for a Tunable X-Band Maser

Center frequency	9.3 Gc
Net gain	20 db min
Electronic gain	30 db
Magnetic Q	90
Number of cavities M	15
Interstage isolation H	0.53 (5.5 db)
Effective single cavity gain g_{oe}	1.26 (2.0 db)
Isolated single cavity gain g_{os}	1.3 (2.3 db)
Tunable bandwidth B_r	0.025 (230 Mc)
Structure bandwidth $\overline{BW}$	0.048 (440 Mc)
Coupling iris susceptance b	3.7
Optimum isolator length	1.04 rad

The general maser design parameters are determined as follows:

1) The electronic gain should be sufficient to overcome the structure loss. The gain-to-loss decibel ratio for operation at 4.2°K is about 6:1, making the electronic gain about 20 per cent higher than the net gain required (in decibels).
2) The magnetic Q of ruby can be obtained from Fig. 8 for the "push-pull" mode at any frequency from 7 to 10 Gc.
3) From B_r, Q_m, and G, the number of cavities M is established from the curves of Fig. 11.
4) Optimum interstage isolation H is determined from O'Meara's Fig. 6 [1].
5) The single cavity gain g_{os} may be found from g_{oe}, H and Fig. 12.
6) The passive structure bandwidth $\overline{BW}$ may then be determined from (7).
7) The coupling iris susceptance b is found from Fig. 7.
8) The optimum isolator length θ_{is} may be obtained from $\theta_{is}+2\tan^{-1}b=\pm\pi/2$.
9) The magnetic field and pump frequency can be determined from the spin-Hamiltonian or from published tables [14].

VII. Cryogenics

The liquid helium dewar (Fig. 15) designed for the coupled-cavity maser is a single fluid type with a fluid capacity of about 6 liters. Radiation protection for the

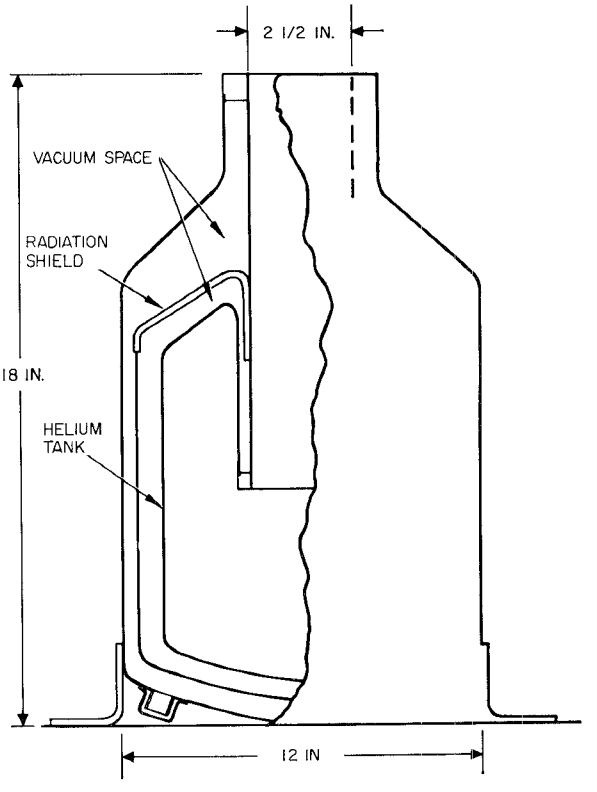

Fig. 15—Cross section of dewar.

liquid helium chamber is provided by a copper shield surrounding the chamber. The shield is connected to the neck of the dewar and during operation is maintained at about 80°K by the helium vapor passing through the neck. The helium chamber and the dewar neck form a re-entrant type structure in which the wall temperature is essentially constant throughout. As a result, the helium liquid does not contact "hot" areas within the dewar with subsequent boil-off, regardless of the position of the dewar. This feature, in addition to the single fluid type dewar permits the dewar to be operated in any angular position from vertical to horizontal.

VIII. Operational Maser Performance

To date, Hughes has developed several masers for systems application in the frequency range of 7600 to 9500 Mc. The operating characteristics of these masers were varied with the application from a net gain of 40 db tunable over 40 Mc/sec to a net gain of 20 db with 200 Mc/sec tunability. The instantaneous 3 db bandwidth ranged from 10 Mc/sec for the high gain masers to 30 Mc/sec for the masers with reduced gain. The noise temperature of the maser is less than 20°K with typical measured values of 12 to 13°K. Measurements of stability indicate a gain drift of less than ± 0.1 db for a period of more than 20 hours of continuous operation, and less than ± 0.2 db when the unit was continuously tilted ± 85 degrees from the vertical.

IX. Conclusions

The coupled resonant cavity type traveling-wave maser has been analyzed as an active microwave filter in this and a companion paper [1], and a design procedure has been established. The important design parameters have been shown which demonstrate the wide range of performance characteristics possible with this type of structure.

The more practical advantages of the coupled-cavity transmission maser over previously reported traveling-wave masers are its reduced size and competitive performance at 4.2°K. These advantages may be particularly important in cases where it is necessary to integrate the maser with mobile equipment or with a closed cycle refrigerator.

References

[1] T. R. O'Meara, "The coupled-cavity transmission maser analysis," IEEE Trans. on microwave theory and technique, vol. MTT 12, pp. 336; January, 1964.
[2] R. W. DeGrasse, E. O. Schultz-DuBois and H. E. D. Scovil, "Three-level solid-state traveling-wave maser," *Bell System Tech. J.*, vol. 38, pp. 305–334; March, 1959.
[3] J. C. Cromack, "A Wide-Tuning Range S-Band Traveling-Wave Maser," Electron Devices Laboratory, Stanford Electronics Laboratory, Stanford, Calif. Tech. Rept., No. 155–5; April, 1963.
[4] G. I. Haddad and J. E. Rowe, "S-band ladder-line traveling-wave maser," IRE Trans. on Microwave Theory and Technique, vol. MTT-10, pp. 3–8; January, 1962.
[5] C. Kittel, "On the theory of ferromagnetic resonance absorption," *Phys. Rev.*, vol. 73, pp. 155–161; January, 1948.
[6] F. Block, "Nuclear induction," *Phys. Rev.*, vol. 70, pp. 460–474; October, 1946.
[7] M. E. Rose, "Magnetic field corrections in the cyclotron," *Phys. Rev.*, vol. 53, pp. 715–719; May, 1938.
[8] P. H. Vartanian, "Research and Development of a Solid State Paramagnetic Maser," Microwave Engineering Laboratories, Inc., AF Cambridge Res. Ctr., Bedford, Mass., Third Quarterly Progress Report on Contract No. AF 19(604)-4071; 10 December 1958 through March 1959.
[9] T. H. Maiman, "Temperature and concentration effects in a ruby maser," in "Quantum Electronics, A Symposium," Columbia University Press, New York, N. Y., pp. 324–327; 1960.
[10] R. Beringer, "Frequency pulling by reactive loads," in "Technique of Microwave Measurements," C. G. Montgomery, Ed., McGraw-Hill Book Co., New York, N. Y., MIT Rad. Lab. Ser., vol. 11, pp. 291–293. 1947,
[11] M. L. Stitch, "Maser amplifier characteristics for transmission and reflection cavities," *J. Appl. Phys.*, vol. 29, pp. 782–789; May, 1958.
[12] G. L. Ragan, "Microwave Transmission Circuits," MIT Rad. Lab. Ser., vol. 9, pp. 653–661; 1948.
[13] F. E. Goodwin and G. E. Moss, "Broadband impedance matching into dielectric filled waveguides," IEEE Trans., on Microwave Theory and Technique, vol. MTT-11, pp. 36–39; January, 1963.
[14] W. S. Chang and A. E. Siegman, "Characteristics of Ruby for Maser Applications," Electron Devices Laboratory, Stanford Electronics Laboratory, Stanford, Calif.; Tech. Rept. No. 156–2; September, 1958.